Article:
Eding, C.B., Köhler, I., Verma, D. et al. (8 more authors) (2021) MTH1 inhibitors for the treatment of psoriasis. Journal of Investigative Dermatology, 141 (8). 2037-2048.e4. ISSN 0022-202X

https://doi.org/10.1016/j.jid.2021.01.026

MTH1 Inhibitors for the Treatment of Psoriasis

JIDOpen

Cecilia Bivik Eding[1,5], Ines Köhler[1,5], Deepti Verma[1], Florence Sjögren[1], Claudia Bamberg[2], Stella Karsten[3], Therese Pham[3], Martin Scobie[3], Thomas Helleday[3,4], Ulrika Warpman Berglund[3] and Charlotta Enerbäck[1]

Inflammatory diseases, including psoriasis, are characterized by changes in redox regulation. The MTH1 prevents the incorporation of oxidized nucleotides during DNA replication. Using MTH1 small-molecule inhibitors, we found induced apoptosis through 8-oxodeoxyguanosine triphosphate accumulation and DNA double-strand breaks after oxidative stress in normal and malignant keratinocytes. In psoriasis, we detected increased MTH1 expression in lesional skin and PBMCs compared with that in the controls. Using the imiquimod psoriasis mouse model, we found that MTH1 inhibition diminished psoriatic histological characteristics and normalized the levels of neutrophils and T cells in the skin and skin-draining lymph nodes. The inhibition abolished the expression of T helper type 17–associated cytokines in the skin, which was in line with decreased levels of IL-17–producing γδ T cells in lymph nodes. In human keratinocytes, MTH1 inhibition prevented the upregulation of IL-17–downstream genes, which was independent of ROS-induced apoptosis. In conclusion, our data support MTH1 inhibition using small molecules suitable for topical application as a promising therapeutic approach to psoriasis.

Journal of Investigative Dermatology (2021) ■, ■–■; doi:10.1016/j.jid.2021.01.026

INTRODUCTION

ROS are produced during normal cellular metabolism and may damage biological macromolecules such as lipids, proteins, and DNA (Valko et al., 2007). To counteract the damaging effects of increased ROS production, cells upregulate antioxidant defense mechanisms, including the human MTH1. MTH1 prevents oxidized nucleotide triphosphates, such as 8-oxodeoxyguanosine triphosphate (8-oxo-dGTP) and 2-hydroxy-2-deoxyadenosine triphosphate (2-OH-dATP), from being incorporated into genomic DNA (Sakumi et al., 1993). This in turn prevents genomic instability, DNA damage, and cell death.

MTH1 expression is induced in cancer cell lines and in a wide range of solid tumors, including breast (Zhang et al., 2017), lung (Fujishita et al., 2017), and colorectal (Koketsu et al., 2004) cancers as a result of increased oxidative pressure by oncogenic stimulation (Liou and Storz, 2010). Moreover, in a variety of cancer types, a significant correlation between MTH1 expression and tumor progression has been observed. For normal cells, MTH1 activity is dispensable (Tsuzuki et al., 2001).

Because MTH1 was identified by the Helleday Laboratory as a potential cancer therapeutic target (Gad et al., 2014), a large number of potent small-molecule inhibitors have been developed through extended pharmacological and biochemical analysis (Gad et al., 2014). MTH1 inhibition effectively and selectively induces cell death in cancer cells by causing a mitotic arrest and the introduction of toxic oxidized nucleotides into genomic DNA (Gad et al., 2019[1], 2014). The use of MTH1 inhibitor (MTH1i) in cancer treatment is currently being evaluated in phase I clinical trials in metastasized solid tumors and hematological cancers. However, whereas MTH1is are a promising treatment, some MTH1is have failed to inhibit cell proliferation through the incorporation of 8-oxo-dGTP into DNA, possibly owing to clinical heterogeneity in cancer tissues and resistance mechanisms (Gad et al., 2014; Warpman Berglund et al., 2016).

Despite the link between altered redox regulation, altered repair responses and DNA damage, and various inflammatory diseases (Chatzinikolaou et al., 2014; Glennon-Alty et al., 2018), the potential of MTH1 inhibition in inflammatory conditions has not yet been evaluated.

It has been suggested that increased levels of ROS contribute to the pathogenesis of psoriasis, a chronic, immune-mediated inflammatory skin disease (Cannavò et al.,

[1]*Ingrid Asp Psoriasis Research Center, Division of Dermatology, Department of Biomedical and Clinical Sciences, Linköping University, Linköping, Sweden;* [2]*Department of Dermatology, Västervik Hospital, Västervik, Sweden;* [3]*Science for Life Laboratory, Department of Oncology-Pathology, Karolinska Institutet, Stockholm, Sweden; and* [4]*Weston Park Cancer Centre, Department of Oncology and Metabolism, University of Sheffield, Sheffield, United Kingdom*

[5]*These authors contributed equally to this work.*

Correspondence: Charlotta Enerbäck, Ingrid Asp Psoriasis Research Center, Department of Biomedical and Clinical Sciences, Linköping University, SE-581 85 Linköping, Sweden. E-mail: charlotta.enerback@liu.se

Abbreviations: 4-HNE, 4-hydroxy-2-nonenal; 7AAD, 7-aminoactinomycin D; 8-oxo-dGTP, 8-oxodeoxyguanosine triphosphate; DOK, dysplastic oral keratinocyte; HEKn, normal human epidermal keratinocyte, neonatal; IMQ, imiquimod; KC, keratinocyte; MTH1i, MTH1 inhibitor; MTH1i-IMQ, MTH1 inhibitor and imiquimod

Received 22 June 2020; revised 19 January 2021; accepted 21 January 2021; accepted manuscript published online XXX; corrected proof published online XXX

[1] Gad H, Mortusewicz O, Rudd SG, Stolz A, Amaral N, Brautigham L, et al. MTH1 promotes mitotic progression to avoid oxidative DNA damage in cancer cells. bioRxiv 2019. doi: https://doi.org/10.1101/575290.

2019; Harden et al., 2015). Although cell control is maintained in psoriasis and the disease is strictly benign, it shares several features with cancer, such as the combination of abnormal differentiation, hyperproliferation, and angiogenesis. This intense cellular activity in the psoriatic skin leads to a local redox imbalance. Furthermore, a systemic redox imbalance in patients with psoriasis has been suggested by significantly increased levels of oxidative stress markers (e.g., malondialdehyde, lipid hydroperoxides, and nitric oxide), reduced levels of antioxidants (e.g., thiols), and a reduction in the activity of antioxidant enzymes (e.g., superoxide dismutase and catalase) (Cannavò et al., 2019; Lin and Huang, 2016; Wagener et al., 2013; Zhang et al., 2019).

In this study, we evaluate an innovative treatment modality for psoriasis that involves the targeting of redox imbalance. Using first-in-class inhibitors against MTH1 (Gad et al., 2014; Warpman Berglund et al., 2016), we demonstrate the proof of concept of oxidative DNA repair inhibitors in a preclinical psoriasis mouse model.

RESULTS

The sensitivity to MTH1 inhibition in keratinocytes correlates with ROS levels

The cell death–inducing potential of five different MTH1is was evaluated in normal human epidermal keratinocytes, neonatal (HEKn) cells (Cascade Biologics, Portland, OR); in precancerous dysplastic oral keratinocyte (DOK) cell line (Sigma-Aldrich, St. Louis, MO); and in the squamous cell carcinoma cell line, A431 (Sigma-Aldrich). The cells were cultured in the presence of 0.01−10 μM MTH1i for 72 hours, and the viability was measured using an MTT viability assay (Figure 1a and b). All the five inhibitors induced a strikingly similar pattern of diminished cell viability. When high concentrations of inhibitors were used, the A431 cells demonstrated a significantly lower viability than seen in HEKn. The DOK cells demonstrated an intermediate level of survival. Normal adult keratinocytes (KCs) and KCs isolated from skin biopsy samples displayed survival comparable with that of the HEKn cells (data not shown).

To determine whether the survival rate correlated with the level of intracellular ROS, we used 4-hydroxy-2-nonenal (4-HNE) staining in immunocytochemistry, which reflects ROS-induced lipid peroxidation. 4-HNE levels were markedly higher in A431 cells than in HEKn cells (Figure 2a).

The incorporation of 8-oxo-dGTP into DNA, leading to cellular apoptosis, is linked to efficient MTH1 inhibition (Warpman Berglund et al., 2016). In line with the survival data, MTH1 inhibition caused a more pronounced accumulation of 8-oxo-dGTP in DNA in A431 cells than in HEKn cells (Figure 2b). In addition, the expression of nuclear 53BP1 (Abcam) foci in A431 cells was increased, which confirms that MTH1 inhibition leads to DNA double-strand breaks in sensitive cells (Figure 2c). Using Annexin V and 7-aminoactinomycin D (7AAD) double staining in flow cytometry, we showed that the fraction of apoptotic cells was markedly increased in A431 cells as compared with that in HEKn cells (Figure 2d).

To evaluate whether increased levels of ROS increase the sensitivity of HEKn to MTH1 inhibition, we treated HEKn with the antioxidant inhibitor, *L*-buthionine sulfoximine (Sigma-Aldrich), which raised intracellular ROS as well as 4-HNE levels in the HEKn (Supplementary Figure S1). The treatment led to significantly reduced viability in HEKn on MTH1 inhibition (Figure 3e). Moreover, ROS augmented the protein level of MTH1 in HEKn cells in a concentration-dependent manner (Figure 2f). *L*-buthionine sulfoximine treatment also resulted in an accumulation of 8-oxo-dGTP, which was further augmented by MTH1 inhibition (Figure 2g). These results show that the apoptosis-inducing potential of the MTH1is in KCs is associated with the severity of the oxidative stress.

MTH1 levels are increased in psoriatic skin and PBMC

To evaluate whether increased levels of ROS in psoriatic lesional tissue may be reflected in elevated levels of MTH1, we analyzed the expression of MTH1 in psoriatic skin and PBMCs. We found an increased *MTH1* mRNA expression in whole-skin biopsies from both lesional and nonlesional psoriatic skin compared with those from control skin (Figure 3a). The upregulation was particularly pronounced in the mRNA from the lesional epidermis compared with that from the normal epidermis (Figure 3b). Furthermore, the levels of MTH1 were increased in PBMCs from patients with psoriasis compared with the levels of MTH1 in cells from controls (Figure 3c). The immunohistochemical staining of MTH1 revealed low expression in nonlesional skin and strong albeit variable expression in the lower parts of the lesional epidermis (Figure 3d). These data support the assumption that targeting these proteins may be a promising anti-inflammatory treatment.

MTH1 inhibition diminishes T helper type 17–driven inflammation in mice

We used the imiquimod (IMQ) mouse model to generate T helper type 17–driven psoriasiform inflammation in mice (van der Fits et al., 2009). After 4 days of daily topical application of IMQ onto the shaved back skin, the severity of the dermatitis was evaluated. Compared with mice treated with only IMQ, mice treated with MTH1i and IMQ (MTH1i-IMQ) demonstrated reduced skin erythema (Figure 4a). A histological examination of the IMQ-treated mice confirmed acanthosis, parakeratosis, and a dermal infiltrate with dilated vessels, which were all significantly reduced by MTH1 inhibition (Figure 4b). Mouse body weight did not change as a result of MTH1 inhibition, suggesting limited severe side effects (data not shown).

The immunofluorescence staining of lesional skin revealed that $CD45^+$ hematopoietic cells were markedly diminished in MTH1i-IMQ–treated mice compared with that in IMQ-treated mice (Figure 4c). Using the neutrophil marker, Ly6B, we found that the $CD45^+$ cells primarily consisted of neutrophils, demonstrating a neutrophil influx in response to IMQ, which was strikingly downregulated by MTH1 inhibition (Figure 4c). The number of $CD3^+$ cells was similar to that in the control skin and in IMQ-treated skin (Figure 4d), which is in line with the reported accumulation of γδ T cells beyond 4 days of IMQ treatment (Tortola et al., 2012). There was a markedly reduced number of $CD3^+$ cells in the skin of MTH1i-IMQ–treated mice, suggesting that T cells may only be sensitive to MTH1 inhibition when activated.

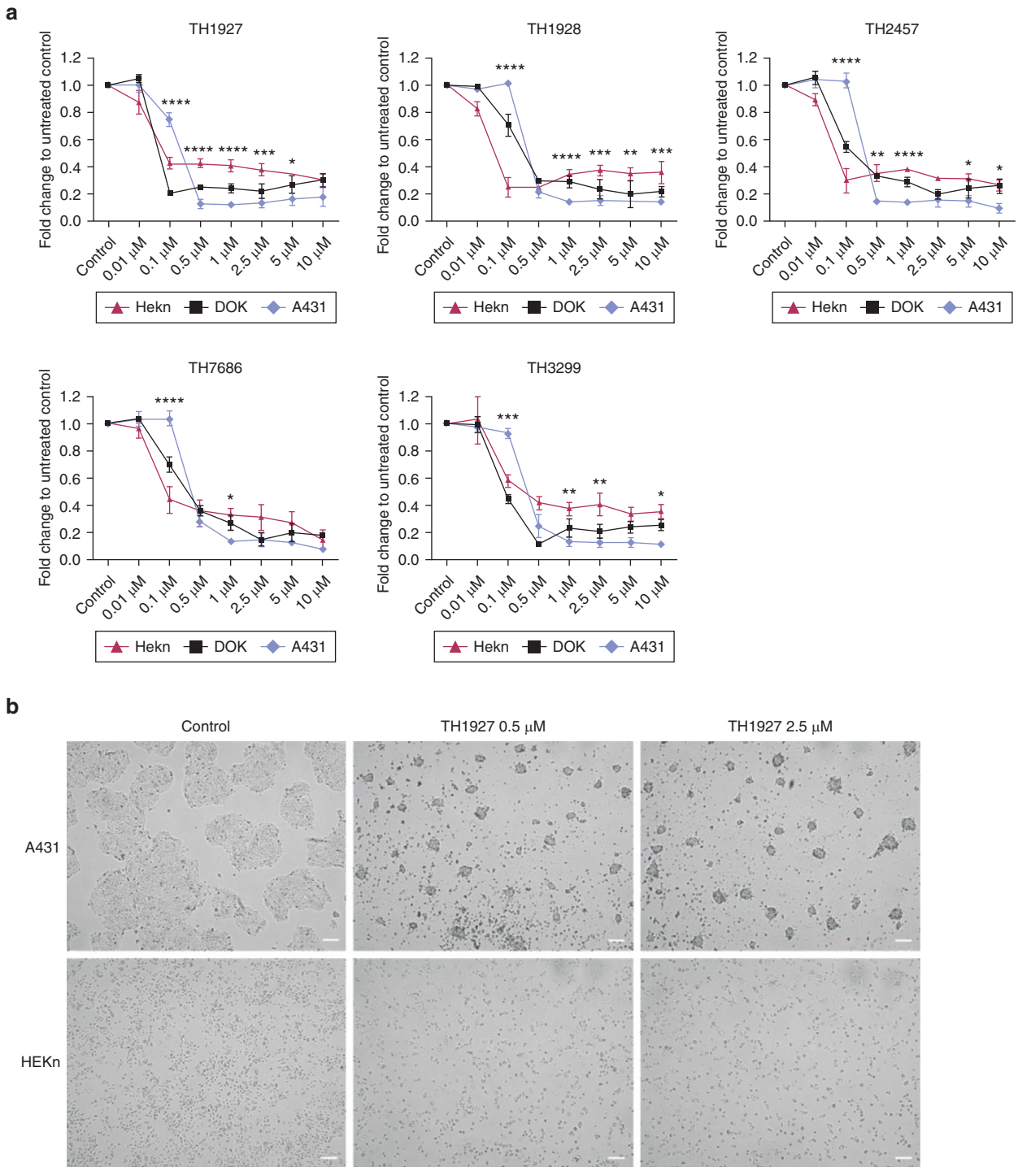

Figure 1. Skin cancer cell lines are more sensitive to MTH1 inhibition than normal KCs (**a**) Viability analyses in HEKn cells, in the A431 human squamous carcinoma cell line, and in the DOK cell line treated with five small-molecule MTH1is (0.01−10 μM; TH1927, TH1928, TH2457, TH7686, and TH3299) for 72 hours. Statistical significances between HEKn and A431 are shown. n = 3−6, *$P < 0.05$, **$P < 0.01$, ***$P < 0.001$, ****$P < 0.0001$. (**b**) Representative photographs of the human squamous carcinoma cell line (A431) and HEKn cells showing the control cells and the cells treated with different concentrations of MTH1i (TH1927). Bar = 200 μm. DOK, dysplastic oral keratinocyte; HEKn, normal human epidermal keratinocytes, neonatal; KC, keratinocyte; MTH1i, MTH1 inhibitor.

In addition, MTH1 inhibition was found to increase the number of oxidized nucleotides, detected with 8-oxo-dGTP staining, in the basal layer of the epidermis in lesional skin (Figure 4e). There was also an increased number of 53BP1 nuclear foci in the epidermal KCs in the skin of MTH1i-IMQ–treated skin, indicating DNA damage (Figure 4f).

We analyzed the mRNA levels of T helper type 17–associated cytokines in the murine skin by qPCR and found a

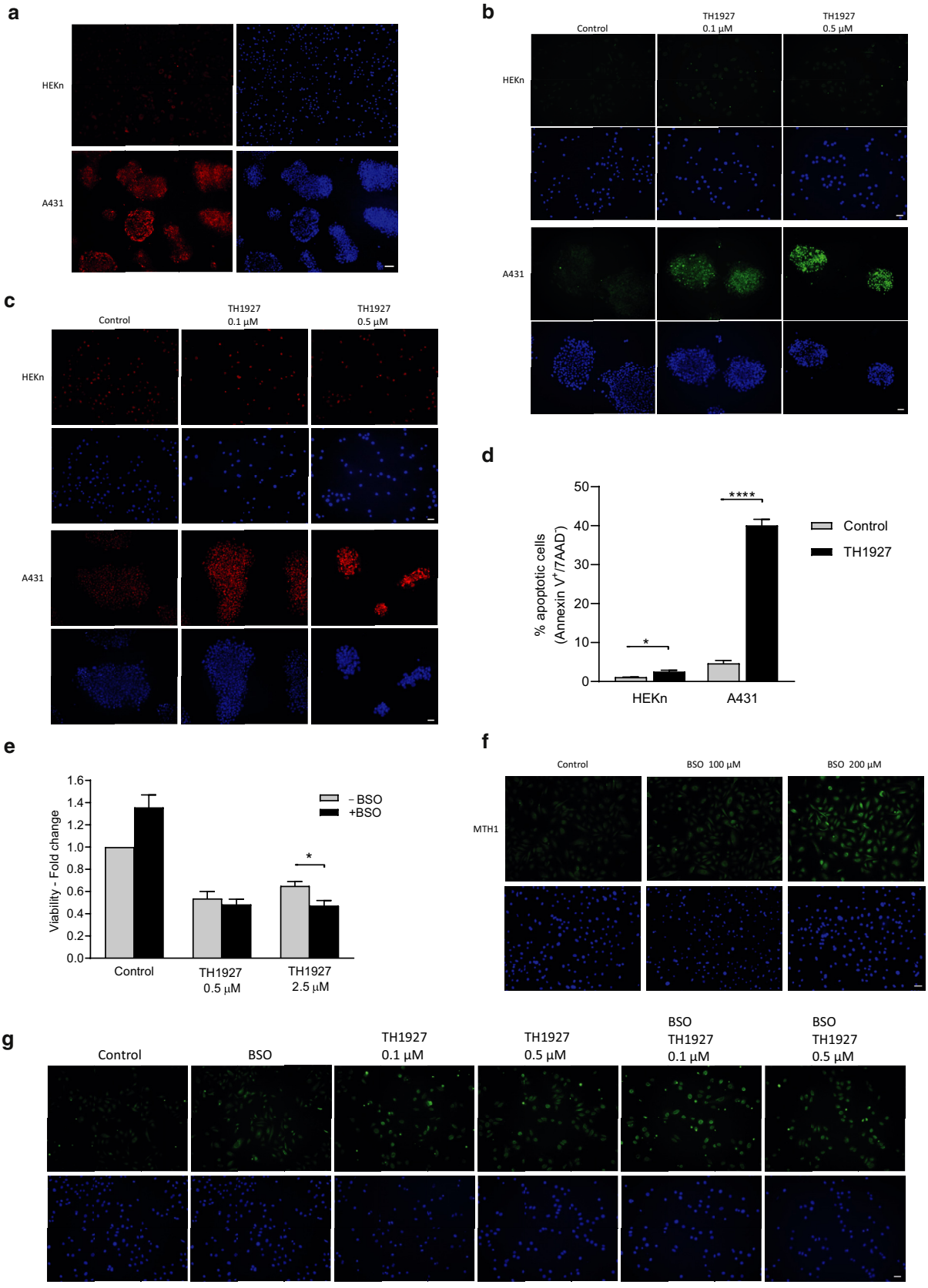

Figure 2. The sensitivity of the MTH1is correlates with the severity of the oxidative stress. (**a**) Increased ROS-induced lipid peroxidation in human squamous carcinoma cells (A431) compared with those in HEKn. 4-HNE staining in immunocytochemistry: red, 4-HNE; blue, DAPI (nuclei). Bar = 100 μm. n = 3. MTH1 inhibition triggers the pronounced accumulation of (**b**) 8-oxo-dGTP and (**c**) 53BP1 induction in the human squamous carcinoma cell line (A431) compared with that in the HEKn cells. Green, 8-oxo-dGTP; red, 53BP1; blue, DAPI (nuclei). Bar = 50 μm. n = 3. (**d**) Flow cytometry analysis of Annexin V and 7AAD expression in the MTH1i (0.5 μM, TH1927)-treated A431 and HEKn. The percentage of early apoptotic cells (Annexin V^+ and $7AAD^-$) is presented. (**e**) An elevated ROS

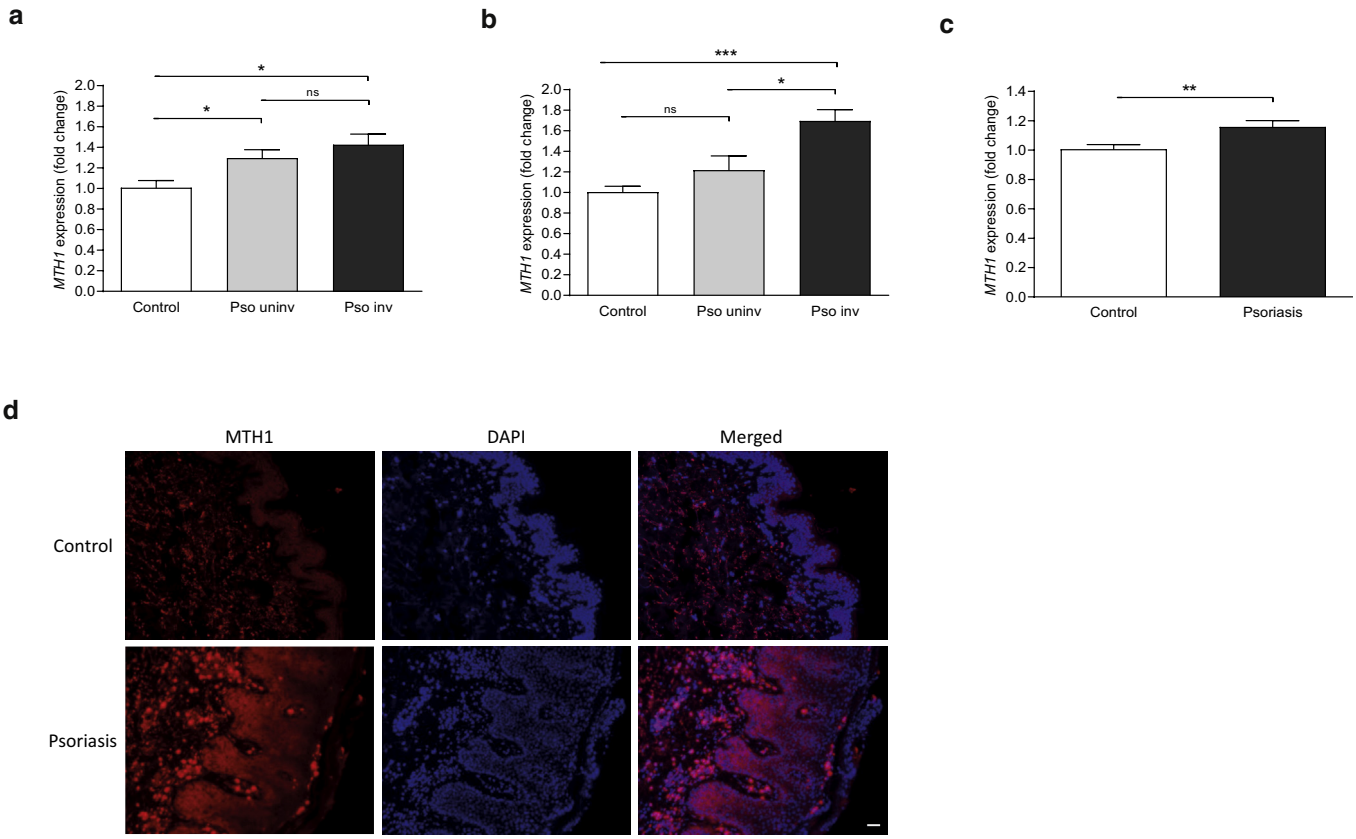

Figure 3. Increased MTH1 expression in psoriatic tissues. *MTH1* mRNA expression analyses of (**a**) whole-skin biopsies (n = 5–8), (**b**) epidermis (n = 5–6) from psoriatic skin (Pso inv, Pso uninv) and control skin, and (**c**) PBMCs (n = 13) from patients and controls. *$P < 0.05$, **$P < 0.01$, ***$P < 0.001$. (**d**) Immunohistochemical MTH1 staining of psoriatic and control skin. Bar = 50 μm; red, MTH1; blue, DAPI (nuclei); n = 6–7. ns, nonsignificant; Pso inv, psoriatic skin involved; Pso uninv, psoriatic skin uninvolved.

complete abolition of *Il-17a* and *Il-22* expression, along with strikingly reduced levels of *Tnf-α* and *Il-23* in MTH1i-IMQ–treated mice compared with that in IMQ-treated mice (Figure 4g). The topical treatment of mice with IMQ resulted in systemic effects on the cellular composition of the spleen, with a shift from lymphoid to myeloid cells (van der Fits et al., 2009). In line with this, IMQ led to spleen enlargement and an increased spleen index (Figure 4h). This was significantly reduced in MTH1i-IMQ–treated mice. Using flow cytometry, we found reduced levels of splenic $CD4^+$ and $CD8^+$ T cells in IMQ-treated mice, and these levels were normalized by MTH1 inhibition (Figure 5a). Similar results were observed in skin-draining lymph nodes (Figure 5b). Interestingly, IMQ dramatically increased the fraction of $Ly6G/C^+$ neutrophils in lymph nodes, but this was reduced to control level by MTH1 inhibition. This result completely confirms our immunohistochemical findings.

The dominant source of IL-17 in IMQ-treated mice is the γδ T cells and, to a lesser extent, the IL-17–producing $CD4^+$ cells (Cai et al., 2011). Using flow cytometry, we analyzed the fraction of IL-17–producing γδ T cells in lymph nodes and found that it was increased by IMQ, which tended to be prevented by MTH1 inhibition (Figure 5c). No significant difference was observed in the IL-17–producing $CD4^+$ cell subset (data not shown). These results show a profound alleviating effect by MTH1 inhibition in IMQ-induced psoriasis-like inflammation.

MTH1 inhibition regulates IL-17–driven inflammation in vitro independently of ROS

The striking downregulation of *Il-17a* and *Il-23* in mouse skin treated with IMQ during MTH1 inhibition prompted us to investigate the putative direct effect of MTH1 inhibition on the IL-17 signaling pathway in KCs. When we treated HEKn cells with IL-17 in combination with TNF-α, the MTH1 protein expression increased (Figure 6a). Furthermore, MTH1 inhibition led to a differential mRNA expression of the IL-17 and IL-22 downstream genes, *CXCL1*, *CXCL5*, *CXCL8*, *S100A8*, and *DEFB4* (Figure 6b and Supplementary Figure S2). The inhibitor TH1927 demonstrated the most

level increases the sensitivity of the HEKn to MTH1 inhibition. The cells were cultured with MTH1i (TH1927; 0.5 μM and 2.5 μM) with or without the glutathione synthesis inhibitor, BSO (100 μM). (**f**) ROS increases MTH1 protein expression in HEKn. The cells were treated for 48 hours with BSO (100 μM and 200 μM). (**g**) ROS induces 8-oxo-dGTP accumulation in HEKn. The KCs were cultured with BSO (200 μM) and MTH1i (TH1927; 0.1 μM and 0.5 μM) for 48 hours. Bar = 50 μm: green, MTH1 and 8-oxo-dGTP; blue, DAPI (nuclei), n = 3. *$P < 0.05$, ****$P < 0.0001$. 4-HNE, 4-hydroxy-2-nonenal; 7ADD, 7-Aminoactinomycin D; 8-oxo-dGTP, 8-oxodeoxyguanosine triphosphate; BSO, *L*-buthionine sulfoximine; HEKn, normal human epidermal keratinocyte, neonatal; KC, keratinocyte; MTH1i, MTH1 inhibitor.

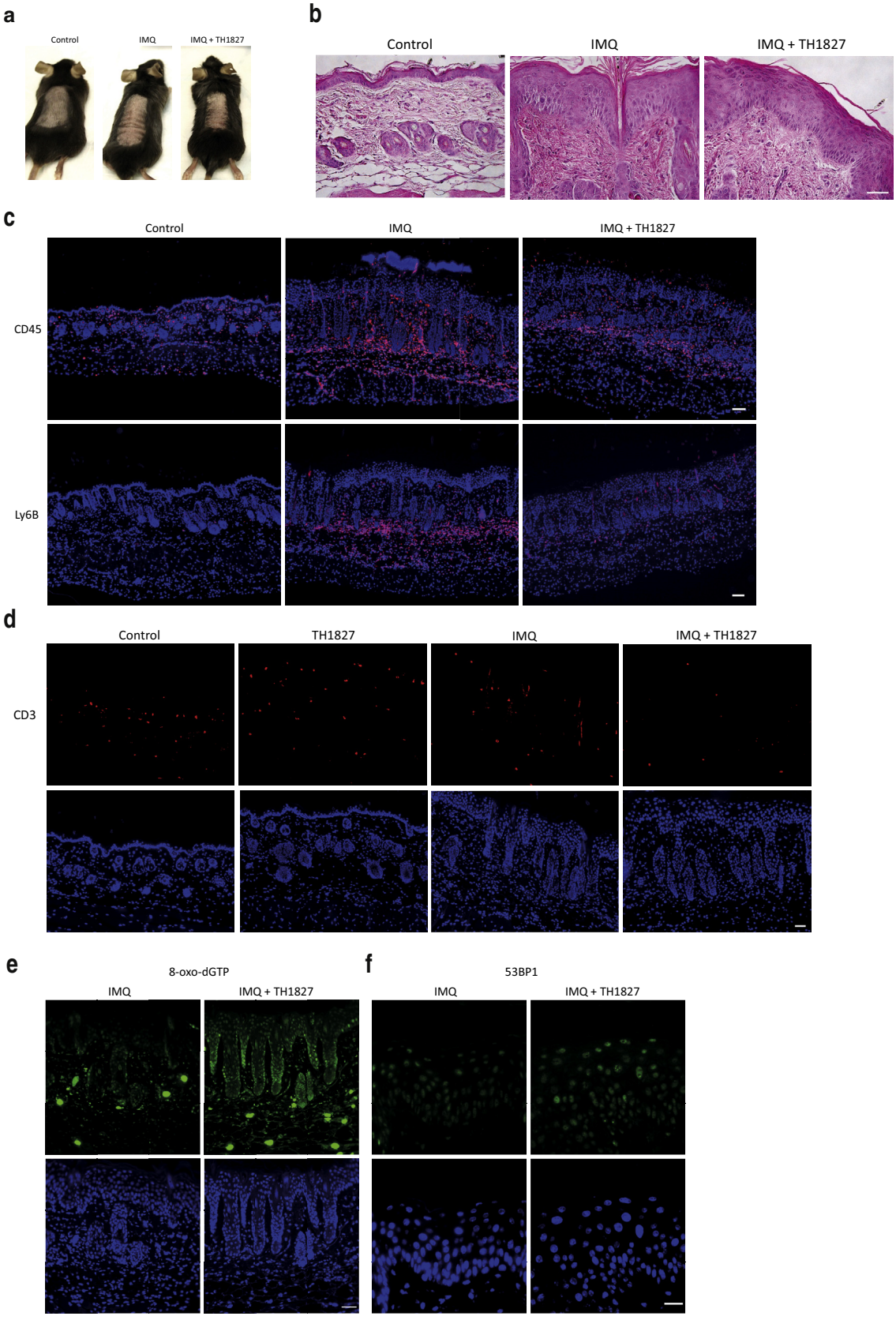

Figure 4. MTH1 inhibition reduces inflammation and increases oxidative damage in IMQ-treated mice. Aldara cream (IMQ) was applied to the shaved backs of mice (C57B6/J) on 4 consecutive days. The mice received a subcutaneous injection (30 mg/kg) of the MTH1i, TH1827, every other day for 5 days (days 1, 3, and 5). n = 6. (**a**) Mice treated with IMQ developed a psoriasis-like skin inflammation with erythema, scaling, and thickening. (**b**) Mice skin stained with H&E. Bar = 100 μm. Immunofluorescence staining (red) of CD45+, (**c**) Ly6B+, and (**d**) CD3+ cells in murine skin. Nuclear counterstaining with DAPI (blue). Bar = 100 μm.

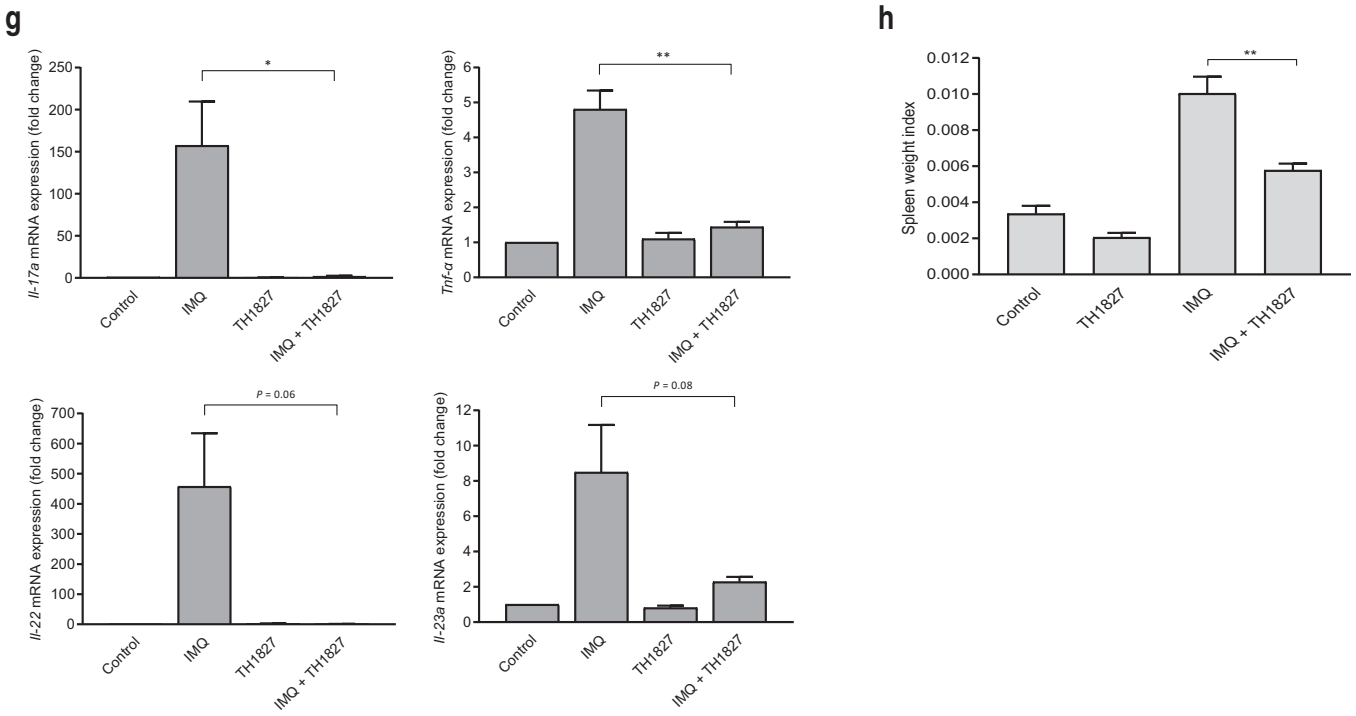

Figure 4. Continued

pronounced decrease in the expression of the chemokines *CXCL1*, *CXCL5*, and *CXCL8* and an increase in the expression of *DEFB4* and *S100A8*. The decrease in *CXCL1* expression in response to MTH1 inhibition was confirmed at the protein level using ELISA (Figure 6c). Interestingly, these results could not be attributed to the reduced survival of cytokine-treated cells because we did not detect higher sensitivity to MTH1 inhibition in the cytokine-treated cells (Supplementary Figure S3a). Using Annexin and 7AAD double staining in flow cytometry, the fraction of apoptotic cells in response to cytokine treatment was unchanged (Supplementary Figure S3b). In agreement with these findings, we did not find any increase in ROS-induced damage (4-HNE levels) in IL-17–treated cells (data not shown). Our data suggest that MTH1 inhibition leads to a direct effect on the IL-17 signaling pathway in KCs, which is not a consequence of ROS-induced cell death.

DISCUSSION

Ongoing ROS production is believed to play an essential role in maintaining chronic inflammation (Chatzinikolaou et al., 2014; Smallwood et al., 2018; Wagener et al., 2013). The activities of infiltrating leukocytes, neutrophils, and macrophages in inflamed tissues result in the enhanced generation of pro-oxidant molecules (Glennon-Alty et al., 2018). Increased protein oxidation and oxidative stress markers have been reported in the lesional skin of patients with psoriasis (Bacchetti et al., 2013; Lee et al., 2017), and a disturbance in the antioxidant defense system has been suggested by increased plasma levels of superoxide dismutase and catalase (Cannavò et al., 2019; Zhang et al., 2019).

In this study, we have evaluated a treatment modality for psoriasis that involves the inhibition of MTH1, resulting in a lack of protection from oxidative damage. We showed that precancerous and skin cancer cell lines were significantly more sensitive to MTH1 inhibition than normal KCs. The apoptosis-inducing potential of MTH1is in KCs correlated with the severity of the oxidative stress. We showed an increase in MTH1 expression in the involved skin and in PBMCs from patients with psoriasis compared with those from the controls, suggesting a potential beneficial effect by MTH1 inhibition.

The effects of MTH1 inhibition on T helper type 17–driven skin inflammation were studied in mice using the potent toll-like receptor 7 ligand, IMQ (van der Fits et al., 2009). IMQ-induced psoriasis is a widely used model for human psoriasis because it is IL-17 and/or IL-23 dependent and produces a phenotype that strongly resembles human psoriasis. We found that the MTH1i, TH1827, reduced psoriatic histological characteristics and strikingly reduced the dermal infiltrate of neutrophils in IMQ-treated mice, which was also observed in mice lymph nodes. Furthermore, the inhibition of MTH1

MTH1 inhibition triggered the nuclear accumulation of (**e**) 8-oxo-dGTP and (**f**) 53BP1 in the epidermis of IMQ-treated skin. Nuclear counterstaining with DAPI. Bar = 50 μm (8-oxo-dGTP) and 25 μm (53BP1). (**g**) Gene expression of the *Il-17a*, *Il-22*, *Il-23*, and *Tnf-α* cytokines in murine skin after MTH1i-IMQ treatment. n = 3, $*P < 0.05$, $**P < 0.01$. (**h**) Spleen index (spleen weight per body weight). n = 3–6, $**P < 0.01$. 8-oxo-dGTP, 8-oxodeoxyguanosine triphosphate; IMQ, imiquimod; MTH1i, MTH1 inhibitor; MTH1i-IMQ, MTH1 inhibitor and imiquimod.

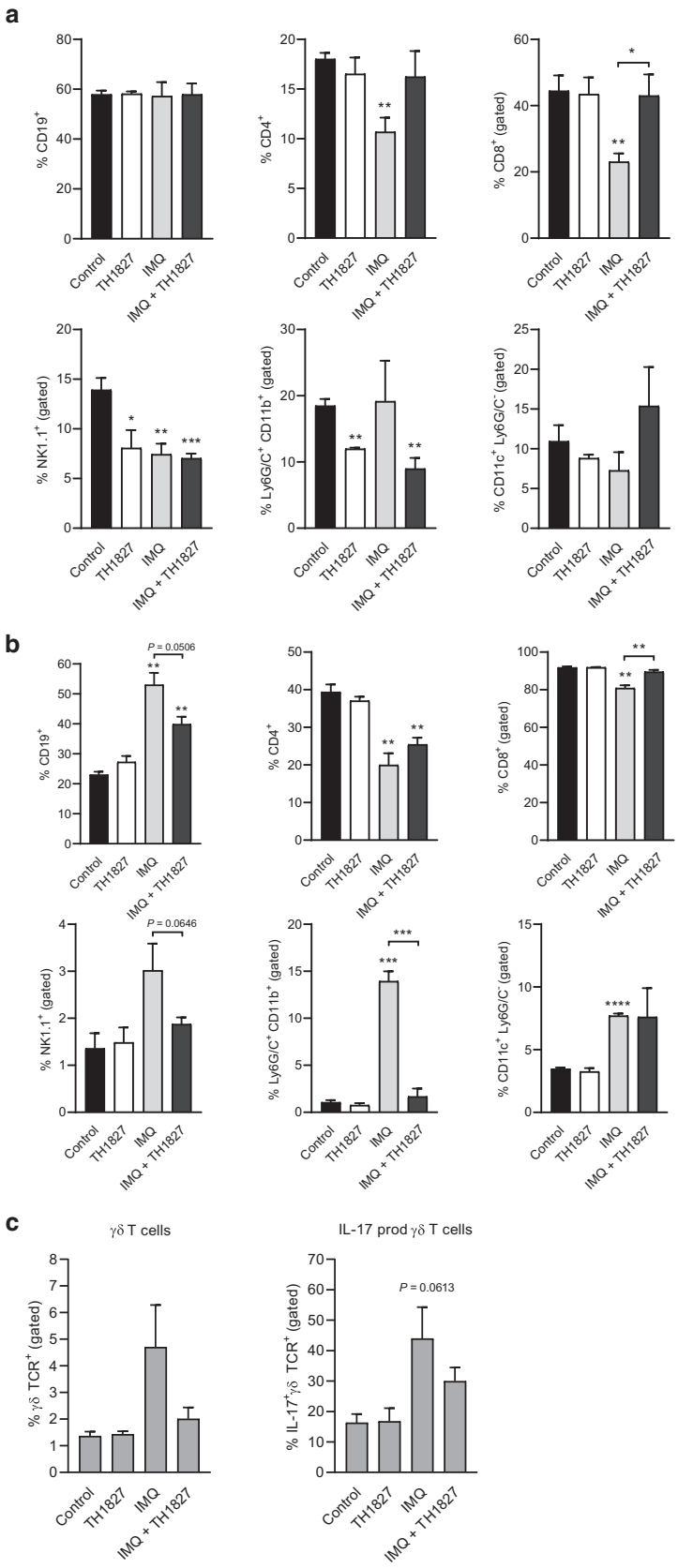

Figure 5. Flow cytometry analyses of mice spleen and skin-draining lymph nodes. Flow cytometry analyses of CD19-, CD4-, CD8-, NK1.1-, Ly6G/C-, and CD11c-expressing cells in mice (**a**) spleen and (**b**) skin-draining lymph nodes and (**c**) γδ T cells and IL-17–expressing γδ T cells in mice lymph nodes. n = 3–6, $*P > 0.05$, $**P < 0.01$, $***P < 0.001$, $****P < 0.0001$ compared with control. IMQ, imiquimod; prod, producing.

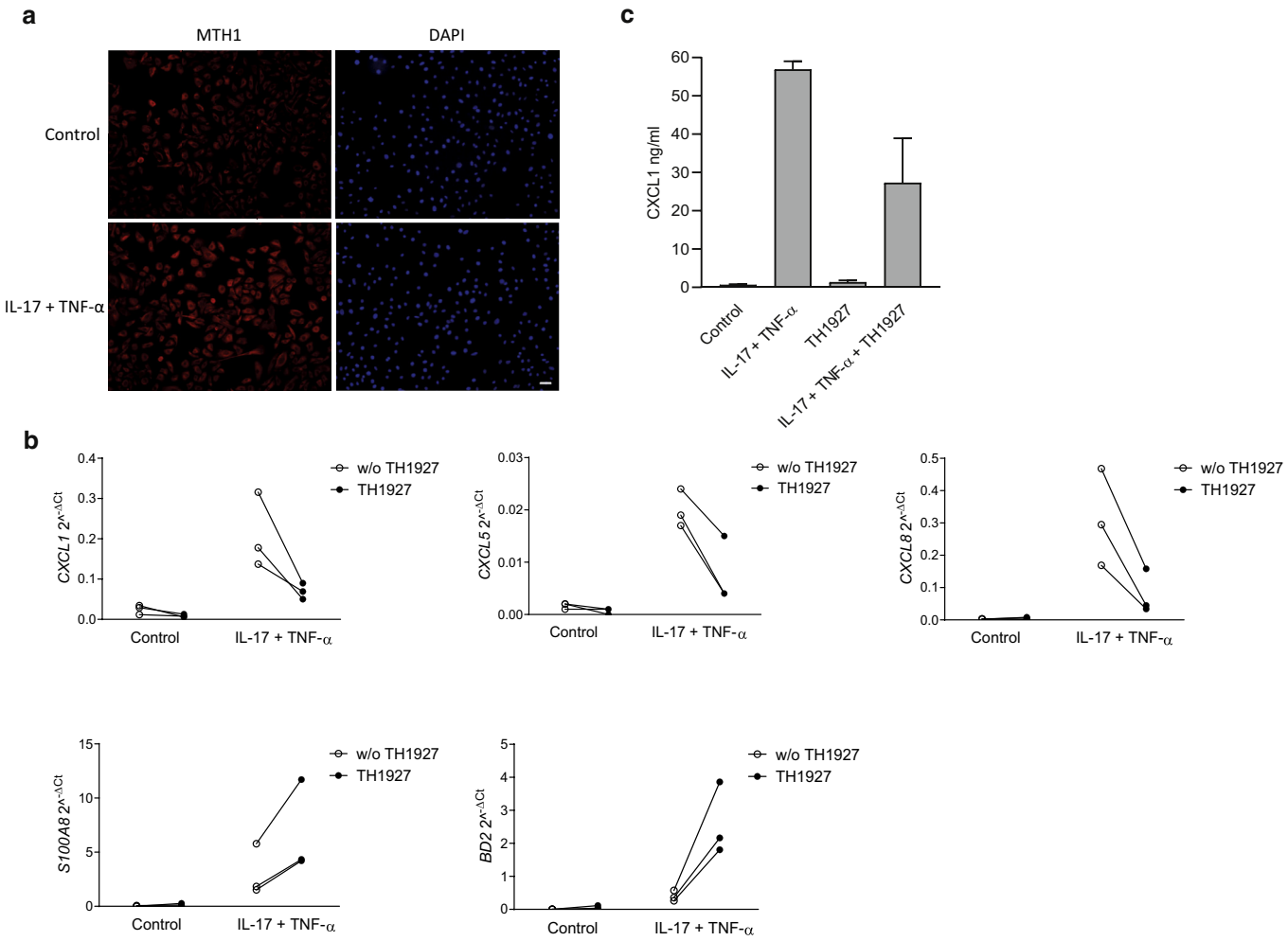

Figure 6. MTH1 regulates IL-17–downstream genes. (**a**) Immunocytochemical staining of MTH1 on HEKn treated with a combination of IL-17 and TNF-α. Nuclear counterstaining with DAPI. Bar = 50 μm. (**b**) Gene expression analyses of *CXCL1*, *CXCL5*, *CXCL8*, *BD2*, and *S100A8* in HEKn pretreated with IL-17A and TNF-α 24 hours before the MTH1i, TH1927 (2.5 μM), was added for 48 hours. n = 3. (**c**) ELISA analysis of CXCL1 protein levels in conditioned media from HEKn after IL-17A and TNF-α and TH1927 treatment. The protein levels are correlated with cell amount. n = 3. HEKn, normal human epidermal keratinocyte, neonatal; MTH1i, MTH1 inhibitor; w/o, without.

almost abolished the expression of T helper type 17–associated cytokines in mouse skin and led to a reduction in the fraction of IL-17–producing γδ T cells in lymph nodes. MTH1i-treated mice also exhibited reduced splenomegaly in response to IMQ, suggesting an effect on systemic inflammation. The MTH1 inhibition led to an accumulation of oxidized nucleotides and an increased expression of 53BP1 in the nuclei of epidermal cells, indicating DNA damage.

Interestingly, we have found that IL-17 increases MTH1 expression and that MTH1 inhibitors prevent the upregulation of IL-17–downstream genes in cultured human KCs. The epidermal recovery after MTH1 inhibition in the mouse model may therefore be a consequence of a direct effect on the KCs rather than solely a secondary effect to the strong reduction in the inflammatory infiltrate. The effect on IL-17–downstream genes was not associated with increased ROS levels and apoptosis, suggesting the presence of an IL-17–modulating effect of MTH1 inhibition, which increases the relevance to the treatment of psoriasis. Moreover, the MTH1-independent effects of the inhibitor cannot be excluded.

In several of the commonly used therapies for psoriasis, such as UV therapy and low-dose methotrexate, the apoptosis of KCs and dermal leukocytes in response to ROS is an important part of their mode of action (Elango et al., 2014; Gu et al., 2015; Vieyra-Garcia and Wolf, 2018). Moreover, TNF-α was shown to induce ROS in KCs (Young et al., 2008), and treatment with the TNF-α inhibitor, etanercept, led to the reduction of lipid peroxidation and an increase in antioxidant capacity (Bacchetti et al., 2013). The inhibition of MTH1, which normally protects cells from oxidative damage, thereby leading to cellular apoptosis, is therefore an interesting modality of treatment for psoriasis.

In conclusion, we have successfully found support for the inhibition of MTH1, implicated in the oxidative stress response, as a treatment modality for psoriasis using small-molecule inhibitors that are suitable for topical application. These are the critical preclinical steps toward clinical trials of

topical treatments that should benefit the majority of patients with mild-to-moderate psoriasis.

MATERIALS AND METHODS

MTH1is

The MTH1is were provided by the Helleday Laboratory, Karolinska Institute, Stockholm, Sweden (WO2014084778).

Isolation of epidermal KCs from human skin biopsies

Punch biopsies (4 mm) from involved and uninvolved psoriatic skin were obtained from patients at the Department of Dermatology at Linköping University Hospital (Sweden), which was approved by the Institutional Review Board at Linköping University (Sweden). All participants had given their written informed consent, and the patients were examined by a dermatologist and were not receiving any systemic treatment.

The biopsies were incubated with 3.8% ammonium thiocyanate for 30 minutes at room temperature or with dispase (2 mg/ml, Roche Diagnostics, Mannheim, Germany) at 4 °C for 18 hours. For qPCR, the epidermis was placed in RLT plus buffer (for further details, see the section on qPCR given later). For KC cell culture, the epidermis was placed in 0.05% trypsin with mechanical disruption for 30 minutes at 37 °C and filtered through a 40-mm nylon cell strainer.

Cells for culture and culture conditions

HEKn cells, the human squamous carcinoma cell line (A431), and the dysplastic oral KC cell line, DOK were cultured according to the recommended procedures. For detailed culture conditions for the cell lines and for KCs isolated from skin biopsies, see the Supplementary Materials and Methods.

Cells were treated with IL-17A (200 ng/ml) in combination with TNF-α (10 ng/ml) (both from R&D Systems, Minneapolis, MN) for 24–48 hours. The following MTH1is were used at concentrations of 0.01–10 μM: TH1927, TH1928, TH2457, TH7686, and TH3299. When indicated, cells were pretreated with cytokines 24 hours before treatment with the MTH1i. The inhibitor of glutathione synthesis, *L*-buthionine sulfoximine (Sigma-Aldrich), was used at concentrations of 50–200 μM.

RNA extraction, cDNA synthesis, and qPCR

Skin harvested from humans and mice was snap frozen in liquid nitrogen and homogenized. RNA was then extracted with the RNeasy Fibrous Tissue Mini Kit (Qiagen, Hilden, Germany) according to the manufacturer's instructions. Cells and epidermis layers were lysed in RLT plus buffer and extracted using the RNeasy Mini Kit (Qiagen).

The Maxima First Strand cDNA Synthesis Kit (Thermo Fisher Scientific, Vilnius, Lithuania) was used for cDNA synthesis. Gene expression was evaluated by qPCR and was performed on a Real-Time 7500 HT System (Applied Biosystems, Foster City, CA) using the TaqMan Fast Advanced Master Mix and predesigned TaqMan Gene expression assays or SYBR green (Applied Biosystems) (Supplementary Materials and Methods). Measurements were performed in triplicate, and expression data were normalized to *RPLP0* endogenous control using the comparative Ct ($2^{-\Delta\Delta Ct}$) method.

Cell viability assay

Cell survival was evaluated after 72 hours of MTH1i treatment using the PrestoBlue Cell Viability Reagent (Life Technologies, Carlsbad, CA) according to the manufacturer's instructions. The optical density readings were measured at 570 and/or 600 nm in a VersaMax Microplate Reader (Molecular Devices, Sunnyvale, CA). All samples were run in triplicate.

Immunofluorescence and immunohistochemistry

Cells were fixed in 4% formaldehyde and permeabilized with 0.1% saponin. They were stained with primary MTH1 (Novus Biologicals, Littleton, CO), 53BP1, or 4-HNE antibodies (both from Abcam, Cambridge, UK) overnight at 4 °C, followed by incubation with secondary Alexa Fluor 488 or 555 conjugated antibody (Molecular Probes, Eugene, OR) for 1 hour at room temperature. For the staining of 8-oxo-dGTP, Alexa 488–conjugated avidin (Life Technologies) was used (Struthers et al., 1998).

For immunohistochemistry, human and mouse skin punch biopsies were fixed and paraffin embedded. The 5 μm sections were deparaffinized in Histolab Clear (Histolab Products, Gothenburg, Sweden) and rehydrated in ethanol. Heat-induced antigen retrieval was performed in a citrate antigen retrieval buffer (pH = 6, Dako, Glostrup, Denmark). After blocking in 5% BSA for 45 minutes at room temperature, the sections were either stained with H&E (Histolab Products) or incubated with primary antibody (Supplementary Materials and Methods) overnight at 4 °C, followed by 1 hour of incubation with Alexa Fluor 555 or 488-conjugated secondary plus antibody. For staining of 8-oxo-dGTP, Alexa 488–conjugated avidin was used. The nuclei were counterstained with DAPI.

Staining was analyzed in an AxioVert.A1 Microscope (Zeiss, Oberkochen, Germany). Negative controls were obtained by omitting the primary antibody, and they displayed no staining.

ELISA

CXCL1 protein levels in conditioned medium were measured using the human CXCL1/GROα Quantikine ELISA Immunoassay Kit (R&D Systems) according to the manufacturer's instructions and were measured in duplicate. The protein levels were correlated with cell amount, and the absorbance was measured in a VersaMax Microplate Reader.

Mouse experiment

C57B6/J female mice were obtained from the Janvier Laboratory (Janvier, Le Genest-St-Isle, France). Animal procedures were performed with the consent of the Institutional Animal Care and Use Committee at Linköping University. The mice received a daily topical application of 62.5 mg Aldara cream (5% IMQ, Meda AB, Solna, Sweden) on a shaved back region (3 × 2 cm) for 4 consecutive days. The mice received a subcutaneous injection (30 mg/kg) of the MTH1i, TH1827, every other day for 5 days (days 1, 3, and 5). The mice were killed on day 5 after 1 hour of the last inhibitor injection. Control mice were sham treated with Vaseline cream (ACO, Kista, Sweden). Skin, spleens, and lymph nodes were collected.

Flow cytometry

Cells from the spleen and lymph node were prepared. The broad immunophenotyping panel used is described in the Supplementary Materials and Methods. Live and/or dead estimation was based on 7AAD or Fixable Viability Stain 510 (BD Biosciences, San Jose, CA) staining. A total of 3–500,000 viable cells in the forward scatter/live gate were collected on FACS ARIA III instrument and analyzed using Kalzua, version 2.1 (Beckman Coulter, Bromma, Sweden), using fluorescence minus one gate. The gating strategy is shown in Supplementary Figure S4.

Cells from lymph nodes were stimulated for 4 hours with 50 ng/ml phorbol 12-myristate 13-acetate (PMA, Sigma-Aldrich) and 1 μg/ml ionomycin (Sigma-Aldrich) in the presence of brefeldin A (BD

Biosciences). The surface staining panel is described in the Supplementary Materials and Methods. Cells were then fixed and permeabilized using BD Cytofix/Cytoperm Fixation/Permeabilization Solution Kit (Gray et al., 2013) according to the manufacturer's instructions and were stained intracellularly with antimouse IL-17A-PE (BD Biosciences). The specificity of intracellular staining was ensured by blocking with unlabeled mAb of the same clone. A total of 50–100,000 viable single $CD3^+$ cells were collected for further analysis by Kalzua, version 2.1 (Supplementary Figure S4).

Apoptosis was analyzed using PE-Annexin V Apoptosis Detection Kit I (BD Biosciences). The dead and damaged cells were detected using 7AAD. The cells were acquired on a Gallios flow cytometer and analyzed using Kaluza software. The Annexin V^- $7AAD^-$ cell population was considered viable.

Statistics

Differences between groups were analyzed using Student's *t*-test in all experiments apart from those analyzing viability in different cell types exposed to MTH1is, where one-way ANOVA followed by Sidak's multiple comparison post-test were performed. $P \leq 0.05$ was considered significant. Statistical analyses were performed using GraphPad Prism, version 8.0.1 (GraphPad Software, San Diego, CA). The data are presented as the mean ± SEM.

Data availability statement

No datasets were generated or analyzed during this study.

ORCIDs

Cecilia Bivik Eding: http://orcid.org/0000-0003-2769-0016
Ines Köhler: http://orcid.org/0000-0002-9260-8528
Deepti Verma: http://orcid.org/0000-0002-7415-2782
Florence Sjögren: http://orcid.org/0000-0002-1630-2447
Claudia Bamberg: http://orcid.org/0000-0002-3978-0572
Stella Karsten: http://orcid.org/0000-0001-6191-4314
Therese Pham: http://orcid.org/0000-0002-5577-6039
Martin Scobie: http://orcid.org/0000-0002-7073-8495
Thomas Helleday: http://orcid.org/0000-0002-7384-092X
Ulrika Warpman Berglund: http://orcid.org/0000-0002-6372-1396
Charlotta Enerbäck: http://orcid.org/0000-0003-1769-3790

CONFLICT OF INTEREST

The Intellectual Property Right of the MTH1 inhibitors in this manuscript is owned by the nonprofit Thomas Helleday Foundation for Medical Research. Oxcia AB is assisting Thomas Helleday Foundation for Medical Research in clinical development. UWB is a board member in Thomas Helleday Foundation for Medical Research and is a shareholder and chairman of the board of Oxcia. TH is the chairman of the board of Thomas Helleday Foundation for Medical Research, a shareholder in Oxcia AB, and an inventor of a patent. MS and TP are shareholders in Oxcia AB, and MS is an inventor of a patent. The remaining authors state no conflict of interest.

ACKNOWLEDGMENTS

This research was supported by grants from the Ingrid Asp Psoriasis Foundation (to CE), the Welander Foundation (to CE), the Swedish Psoriasis Association (to CE), the Swedish Cancer Society CAN-18-0658 (to TH), Svenska Smärtafonden (to TH), and Swedish Foundation for Strategic Research RB13-0224 (to UWB). We acknowledge Annika Lindquist, Uppsala University Drug Optimization and Pharmaceutical Profiling Platform, Uppsala University (Sweden) for analysis of compound concentration in tissue.

AUTHOR CONTRIBUTIONS

Conceptualization: TH, UWB, CE; Formal Analysis: CBE, IK, DV, FS; Funding Acquisition: CE, TH; Investigation: CBE, IK, DV, FS, MS, TP, SK, TH, UWB; Methodology: CBE, IK, DV, FS; Resources: TH, UWB, MS, CB, TP, SK; Writing - Original Draft Preparation: CBE, IK, CE; Writing - Review and Editing: CBE, IK, DV, FJ, CB, SK, TP, MS, TH, UWB, CE

SUPPLEMENTARY MATERIAL

Supplementary material is linked to the online version of the paper at www.jidonline.org, and at https://doi.org/10.1016/j.jid.2021.01.026.

REFERENCES

Bacchetti T, Campanati A, Ferretti G, Simonetti O, Liberati G, Offidani AM. Oxidative stress and psoriasis: the effect of antitumour necrosis factor-alpha inhibitor treatment. Br J Dermatol 2013;168:984–9.

Cai Y, Shen X, Ding C, Qi C, Li K, Li X, et al. Pivotal role of dermal IL-17-producing γδ T cells in skin inflammation. Immunity 2011;35:596–610.

Cannavò SP, Riso G, Casciaro M, Di Salvo E, Gangemi S. Oxidative stress involvement in psoriasis: a systematic review. Free Radic Res 2019;53:829–40.

Chatzinikolaou G, Karakasilioti I, Garinis GA. DNA damage and innate immunity: links and trade-offs. Trends Immunol 2014;35:429–35.

Elango T, Dayalan H, Gnanaraj P, Malligarjunan H, Subramanian S. Impact of methotrexate on oxidative stress and apoptosis markers in psoriatic patients. Clin Exp Med 2014;14:431–7.

Fujishita T, Okamoto T, Akamine T, Takamori S, Takada K, Katsura M, et al. Association of MTH1 expression with the tumor malignant potential and poor prognosis in patients with resected lung cancer. Lung Cancer 2017;109:52–7.

Gad H, Koolmeister T, Jemth AS, Eshtad S, Jacques SA, Ström CE, et al. MTH1 inhibition eradicates cancer by preventing sanitation of the dNTP pool. Nature 2014;508:215–21.

Glennon-Alty L, Hackett AP, Chapman EA, Wright HL. Neutrophils and redox stress in the pathogenesis of autoimmune disease. Free Radic Biol Med 2018;125:25–35.

Gray EE, Ramírez-Valle F, Xu Y, Wu S, Wu Z, Karjalainen KE, et al. Deficiency in IL-17-committed Vγ4(+) γδ T cells in a spontaneous Sox13-mutant CD45.1(+) congenic mouse substrain provides protection from dermatitis. Nat Immunol 2013;14:584–92.

Gu X, Nylander E, Coates PJ, Nylander K. Oxidation reduction is a key process for successful treatment of psoriasis by narrow-band UVB phototherapy. Acta Derm Venereol 2015;95:140–6.

Harden JL, Krueger JG, Bowcock AM. The immunogenetics of Psoriasis: a comprehensive review. J Autoimmun 2015;64:66–73.

Koketsu S, Watanabe T, Nagawa H. Expression of DNA repair protein: MYH, NTH1, and MTH1 in colorectal cancer. Hepatogastroenterology 2004;51:638–42.

Lee YJ, Bae JH, Kang SG, Cho SW, Chun DI, Nam SM, et al. Pro-oxidant status and Nrf2 levels in psoriasis vulgaris skin tissues and dimethyl fumarate-treated HaCaT cells. Arch Pharm Res 2017;40:1105–16.

Lin X, Huang T. Oxidative stress in psoriasis and potential therapeutic use of antioxidants. Free Radic Res 2016;50:585–95.

Liou GY, Storz P. Reactive oxygen species in cancer. Free Radic Res 2010;44:479–96.

Sakumi K, Furuichi M, Tsuzuki T, Kakuma T, Kawabata S, Maki H, et al. Cloning and expression of cDNA for a human enzyme that hydrolyzes 8-oxo-dGTP, a mutagenic substrate for DNA synthesis. J Biol Chem 1993;268:23524–30.

Smallwood MJ, Nissim A, Knight AR, Whiteman M, Haigh R, Winyard PG. Oxidative stress in autoimmune rheumatic diseases. Free Radic Biol Med 2018;125:3–14.

Struthers L, Patel R, Clark J, Thomas S. Direct detection of 8-oxodeoxyguanosine and 8-oxoguanine by avidin and its analogues. Anal Biochem 1998;255:20–31.

Tortola L, Rosenwald E, Abel B, Blumberg H, Schäfer M, Coyle AJ, et al. Psoriasiform dermatitis is driven by IL-36-mediated DC-keratinocyte crosstalk. J Clin Invest 2012;122:3965–76.

Tsuzuki T, Egashira A, Kura S. Analysis of MTH1 gene function in mice with targeted mutagenesis. Mutat Res 2001;477:71–8.

Valko M, Leibfritz D, Moncol J, Cronin MT, Mazur M, Telser J. Free radicals and antioxidants in normal physiological functions and human disease. Int J Biochem Cell Biol 2007;39:44–84.

van der Fits L, Mourits S, Voerman JS, Kant M, Boon L, Laman JD, et al. Imiquimod-induced psoriasis-like skin inflammation in mice is mediated via the IL-23/IL-17 axis. J Immunol 2009;182:5836–45.

Vieyra-Garcia PA, Wolf P. From early immunomodulatory triggers to immunosuppressive outcome: therapeutic implications of the complex interplay

between the wavebands of sunlight and the skin. Front Med (Lausanne) 2018;5:232.

Wagener FA, Carels CE, Lundvig DM. Targeting the redox balance in inflammatory skin conditions. Int J Mol Sci 2013;14:9126–67.

Warpman Berglund U, Sanjiv K, Gad H, Kalderén C, Koolmeister T, Pham T, et al. Validation and development of MTH1 inhibitors for treatment of cancer. Ann Oncol 2016;27:2275–83.

Young CN, Koepke JI, Terlecky LJ, Borkin MS, Boyd SL, Terlecky SR. Reactive oxygen species in tumor necrosis factor-alpha-activated primary human keratinocytes: implications for psoriasis and inflammatory skin disease [published correction appears in J Invest Dermatol 2009;129:1838]. J Invest Dermatol 2008;128:2606–14.

Zhang X, Song W, Zhou Y, Mao F, Lin Y, Guan J, et al. Expression and function of MutT homolog 1 in distinct subtypes of breast cancer. Oncol Lett 2017;13:2161–8.

Zhang Y, Li Z, Ma Y, Mu Z. Association of total oxidant status, total antioxidant status, and malondialdehyde and catalase levels with psoriasis: a systematic review and meta-analysis. Clin Rheumatol 2019;38:2659–71.

SUPPLEMENTARY MATERIALS AND METHODS

Cells for culture and culture conditions

Normal human epidermal neonatal keratinocytes, neonatal cells were cultured in a complete EpiLife medium supplemented with 1% EpiLife defined growth supplement and calcium chloride (0.06 μM; all from Cascade Biologics, Portland, OR). The human squamous carcinoma cell line, A431 (Sigma-Aldrich, St. Louis, MO), was grown in MEM, supplemented with 10% fetal bovine serum (Gibco, Gaithersburg, MD), 2 mM L-glutamine (Gibco), and 1% MEM nonessential amino acids (Sigma-Aldrich). The dysplastic oral KC cell line (Sigma-Aldrich) was cultured in DMEM supplemented with 10% fetal bovine serum, 2 mM L-glutamine, and 5 μg/ml hydrocortisone (Sigma-Aldrich). KCs isolated from skin biopsies were cultured in KC serum–free medium with L-glutamine supplemented with 25 μg/ml bovine pituitary extract and 1 ng/ml EGF (Gibco). All the media also contained 1% amphotericin B (Gibco) and 1% penicillin and streptomycin (Lonza, Verviers, Belgium).

RNA extraction, cDNA synthesis, and qPCR

The following predesigned TaqMan Gene expression assays (Applied Biosystems, Foster City, CA) were used: *CXCL1* (Hs00236937_m1), *CXCL5* (Hs01099660_g1), *CXCL8* (Hs00174103_m1), *S100A8* (Hs00374264_g1), *BD2* (Hs00175474_m1), and *RPLP0* (Hs99999902_m1) for human expression and *Il-17a* (Mm00439618_m1), *Il-22* (Mm01226722_g1), *Il-23a* (Mm00518984_m1), *Tnf-α* (Mm00443258_m1), and *Rplp0* (Mm00725448_s1) for mouse expression. SYBR green (Applied Biosystems) was used for the expression analysis of MTH1 using the following primer sequences: *MTH1*: forward 5′-GTGCAGAACCCAGGGACCAT-3′ and reverse 5′-GCCCACGAACTCAAACACGA-3′ (Gad et al., 2014) and *RPLP0*: forward 5′-ACTGTGCCAGCCCAGAACA-3′ and reverse 5′-AGCCTGGAAAAAGGAGGTCTT-3′.

Immunohistochemistry

The following primary antibodies were used: CD45 (Abcam, Cambridge, United Kingdom), Ly6B.2 (Novus Biologicals, Littleton, CO), CD3 (Abcam), MTH1 (Novus Biologicals), and 53BP1 (Abcam).

Flow cytometry

The broad immunophenotyping panel included antimouse CD8-AlexaFlour700, CD11b-APC, CD11c-BrilliantViolet 421, Ly6G/C-BrilliantViolet 786, and NK1.1-PECy7 (all from BD Biosciences, San Jose, CA), CD19-FITC (from Nordic Biosite, Stockholm, Sweden), and anti–CD4-PECy5.5 (eBioscience, San Diego, CA).

For the IL-17A staining of the lymph nodes, surface staining with antimouse CD11b-BrilliantViolet 650, CD3-PECF594, and γδ TCR-BrilliantViolet 421 (all from BD Biosciences); anti–CD196-BrilliantViolet 786 and anti–CD19-FITC (Nordic Biosite); and anti–CD4-PECy5.5 (eBioscience) was first performed. Anti-mouse IL-17A—PE (BD Biosciences) was used for intracellular staining.

SUPPLEMENTARY REFERENCE

Gad H, Koolmeister T, Jemth AS, Eshtad S, Jacques SA, Ström CE, et al. MTH1 inhibition eradicates cancer by preventing sanitation of the dNTP pool. Nature 2014;508:215–21.

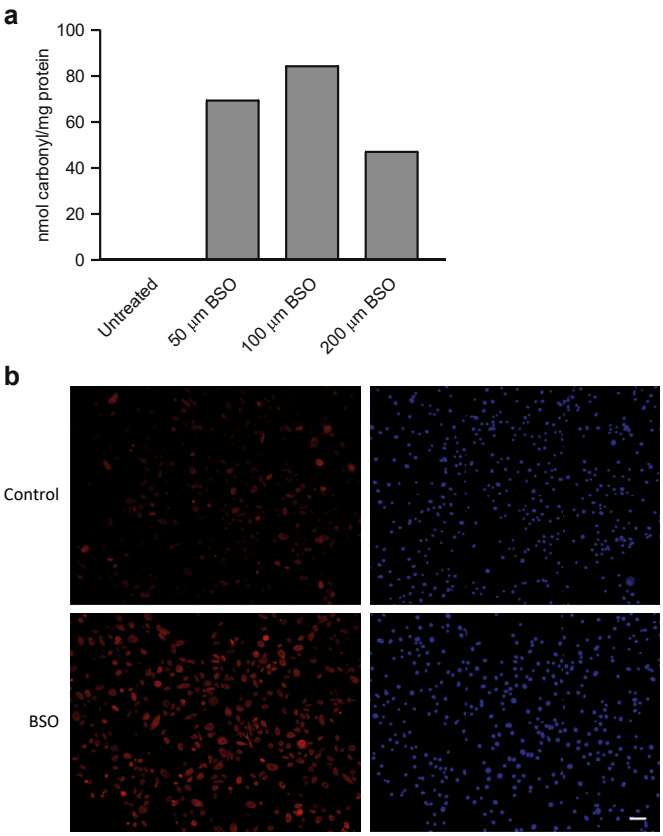

Supplementary Figure S1. Treatment with antioxidant inhibitor results in increased ROS and lipid peroxidation in KCs. Incubation with the glutathione synthesis inhibitor, BSO (50–200 μM), resulted in increased (**a**) ROS levels (n = 1) and (**b**) 4-HNE (n = 3) immunocytochemical staining in HEKn. Red, 4-HNE; blue, DAPI (nuclei). Bar = 100 μm. 4-HNE, 4-hydroxy-2-nonenal; BSO, *L*-buthionine sulfoximine; HEKn, normal human epidermal keratinocyte, neonatal; KC, keratinocyte.

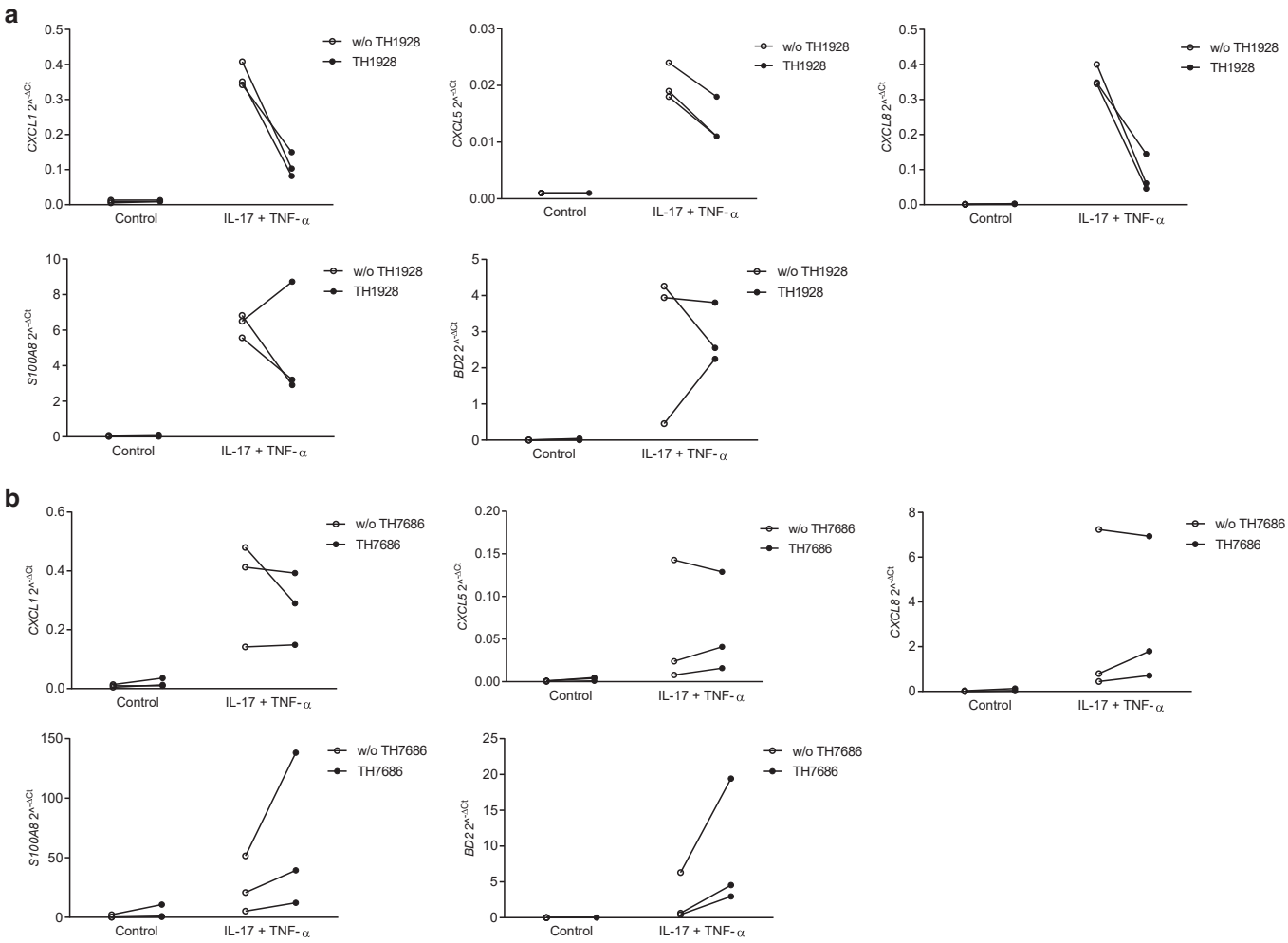

Supplementary Figure S2. MTH1 regulates IL-17–downstream genes. Gene expression analyses of *CXCL1*, *CXCL5*, *CXCL8*, *BD2*, and *S100A8* in HEKn pretreated with IL-17A and TNF-α 24 hours before the MTH1i (**a**) TH1928 (2.5 μM) or (**b**) TH7686 (2.5 μM) was added for 48 hours. n = 3. HEKn, normal human epidermal keratinocyte, neonatal; MTH1i, MTH1 inhibitor; w/o, without.

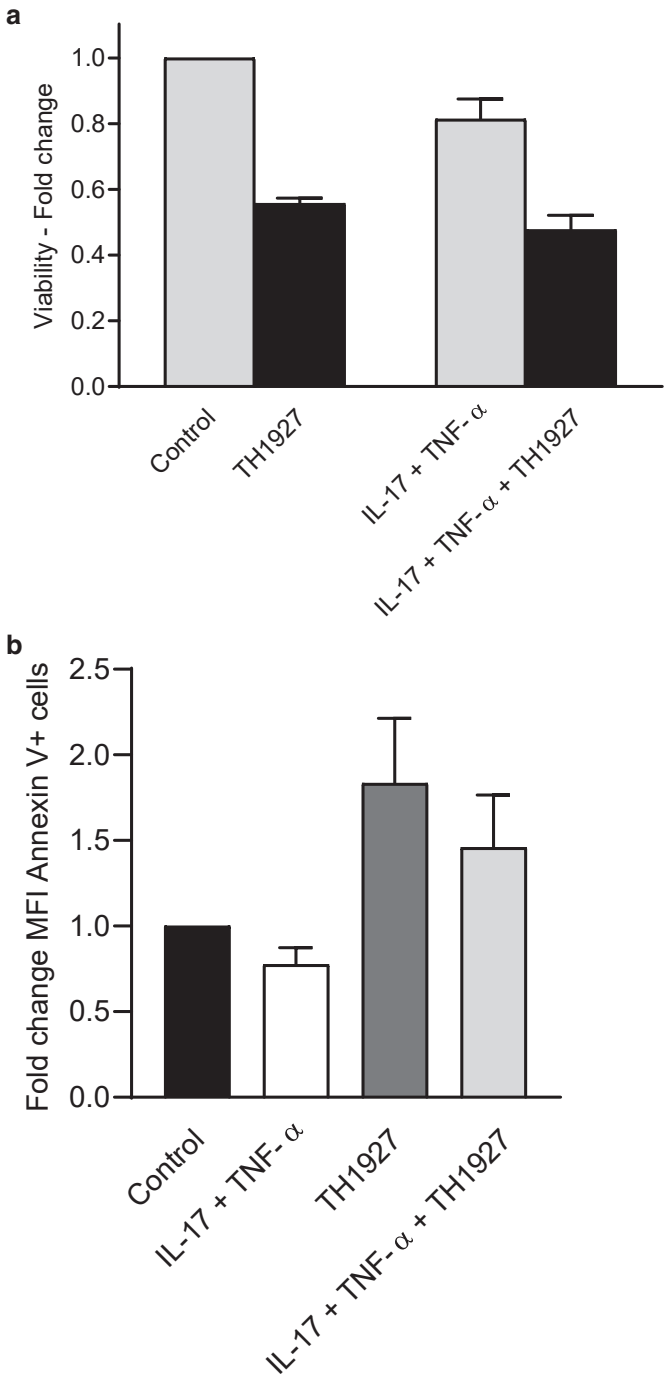

Supplementary Figure S3. Cytokine treatment does not increase sensitivity to MTH1 inhibition. HEKn were cultured with a combination of IL-17A and TNF-α for 24 hours before MTH1i (TH3299, 2.5 μM) treatment for 48 hours. (**a**) Viability was measured with a PrestoBlue viability assay. n = 3. (**b**) Flow cytometry analysis of Annexin V expression. n = 3. HEKn, normal human epidermal keratinocyte, neonatal; MFI, median fluorescence intensity; MTH1i, MTH1 inhibitor.

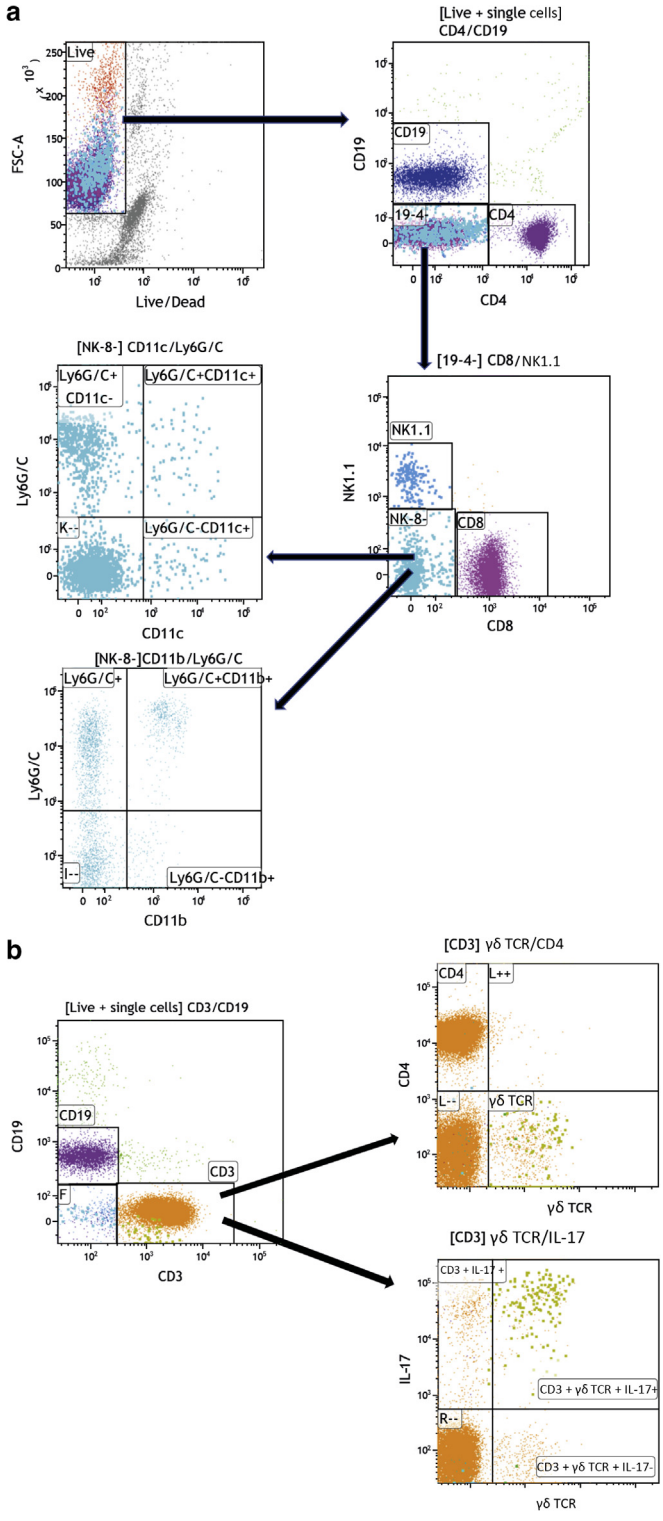

Supplementary Figure S4. Gating strategies for flow cytometry analyses. Gating strategies for immunophenotyping of cells from (**a**) lymph node and spleen tissues, and (**b**) lymphocyte intracellular staining of the lymph nodes. FSC-A, forward scatter area.